JOURNAL OF CATALYSIS **172,** 238–242 (1997)
ARTICLE NO. CA971866

RESEARCH NOTE

Reaction Mechanism of Methanol Synthesis from Carbon Dioxide and Hydrogen on Ceria-Supported Palladium Catalysts with SMSI Effect

Li Fan[1] and Kaoru Fujimoto

Department of Applied Chemistry, School of Engineering, The University of Tokyo, Hongo, Bunkyo-ku, Tokyo, 113, Japan

Received November 18, 1996; revised July 7, 1997; accepted August 14, 1997

Strong metal-support interaction (SMSI) was first claimed by Tauster *et al.* (1, 2) to interpret the diminished H_2 and CO chemisorption on titania-supported platinum group metals reduced above 700 K. Since then a large volume of literature about the SMSI effect has been reported in the past decade (3–5). It has been found that SMSI can enhance reaction activity involving hydrogenation of CO and carbonyl bonds.

On ceria, oxygen is adsorbed reversibly because of its small electric potential (1.7 V) between Ce^{3+} and Ce^{4+} redox couple. Ceria is widely regarded as a kind of oxygen-tank to adjust oxygen concentration at the catalyst surface under reaction condition. It is expected that SMSI can appear on the ceria-supported noble metal catalysts. Several reports declared SMSI phenomenon on Pt/CeO_2 (6) and Rh/CeO_2 (7). Also Zafiris and Gorte (8) reported that lattice oxygen in ceria could be activated by Rh in Rh/CeO_2 catalysts. We designed the high-temperature-reduced Pd/CeO_2 catalysts and it is expected that SMSI on this catalyst system can activate CO_2 through active surface oxygen species.

Catalytic hydrogenation of carbon dioxide into valuable chemicals and fuels such as methanol has been recently recognized as one of the promising recycle technologies for emitted CO_2. Under atmospheric pressure, hydrogenation of CO_2 on supported Pd catalysts produced only methane and CO (9, 10). In most cases, methane is not the favored preduct in hydrogenation of CO_2, due to its stronger greenhouse effect than that of carbon dioxide. We found that a Pd/CeO_2 catalyst reduced with hydrogen at 500°C exhibited high activity and long lifetime for methanol synthesis from CO_2 and H_2 (11). This article aims to elucidate the SMSI mechanism in this catalytic system.

The preparation method of the Pd/CeO_2 catalyst and the reaction conditions were described in the previous report (11). Temperature programmed desorption (TPD) of adsorbed CO_2 was carried out in helium. Also temperature programmed surface reaction (TPSR) of the adsorbed CO_2 was conducted in flowing hydrogen.

X-ray photoelectron spectra (XPS) were acquired on a VG ESCALAB 220-1 Multi-Technique Surface Analysis System equipped with a pretreatment chamber. Measured binding energies were adjusted with respect to the C_{1s} peak. In order to ensure identical surface conditions as those in the catalytic reaction, these samples (after passivation) were reduced in a glass cell connected to the vacuum system. After reduction and evacuation, the samples were sealed in the glass cell. In the glove box filled with N_2, these samples were then transported in an O-ring-sealed transfer vessel to the XPS pretreatment chamber, without exposure to the atmosphere. X-ray diffraction was conducted on Rigaku instrument (RAD-1B, CuK_α). The Scherrer equation was used to determine the average palladium particle size.

As summarized in Table 1, XPS data indicate that the binding energy of Pd was the same for both 400°C-reduced (LTR) and 500°C-reduced (HTR) catalyst, but lower than that of Pd^0 state. The supported Pd on both catalysts should be at electron-rich state, accepting the electrons from CeO_x. This phenomenon is in accordance to the observation of Bell *et al.* for Pd/La_2O_3 (12). Concerning Ce, as shown in Fig. 1, two large peaks (885.0, 903.8 eV) appeared on 400°C-reduced catalyst, accompanied by three small peaks (881.6, 898.5, 916.2 eV). Being confirmed in several literature studies (13, 14), two peaks (885.0, 903.8 eV) are specified to Ce^{4+} and three peaks (881.6, 898.5, 916.2 eV) are attributed to Ce^{3+}. Conversely, these three small peaks (881.6, 898.5, 916.2 eV) increased sharply for 500°C-reduced catalyst while other two peaks (885.0, 903.8 eV), correspondingly, diminished remarkably.

More interestingly, binding energy peaks of O_{1s} converted from 532.0 eV (main) + 529.6 eV (shoulder) on 400°C-reduced catalyst to 532.0 eV (shoulder) + 529.6 eV (main) on 500°C-reduced catalyst. The 532.0 eV peak

[1] Corresponding author. E-mail: tfan@hongo.ecc.u-tokyo.ac.jp.

0021-9517/97 $25.00

TABLE 1

XPS Results of Pd/CeO_2 Catalysts

	Reduction temp.	B. E. (eV)	FWHM (eV)	
$Pd_{3d5/2}$	400°C	334.8	4.0	
	500°C	334.8	3.2	
Pd^0 B. E. = 335.1–335.5 eV				
	Reduction temp.	B. E. (eV)		
Ce_{3d}	400°C	885.0	903.8	
	500°C	881.6	898.5	916.2
Only main peaks of cerium are listed				
	Reduction temp.		B. E. (eV)	
O_{1s}	400°C		532.0	
	500°C		529.6	
Only main peaks of cerium are listed				
	Reduction temp.		Pd_{3d}/Ce_{3d} ratio	
Pd_{3d}/Ce_{3d} ratio	400°C		0.254	
	500°C		0.023	

belongs to CeO_2 and the 529.6 eV peak refers to Ce_2O_3. It is clearly displayed here that CeO_2 transferred to Ce_2O_3, when the reduction temperature was increased from 400 to 500°C. Information from O_{1s} XPS signals is in good accordance to Ce peak change in XPS.

Also from *in situ* XPS measurement, the surface concentration of Pd and Ce can be determined from the peak ratio

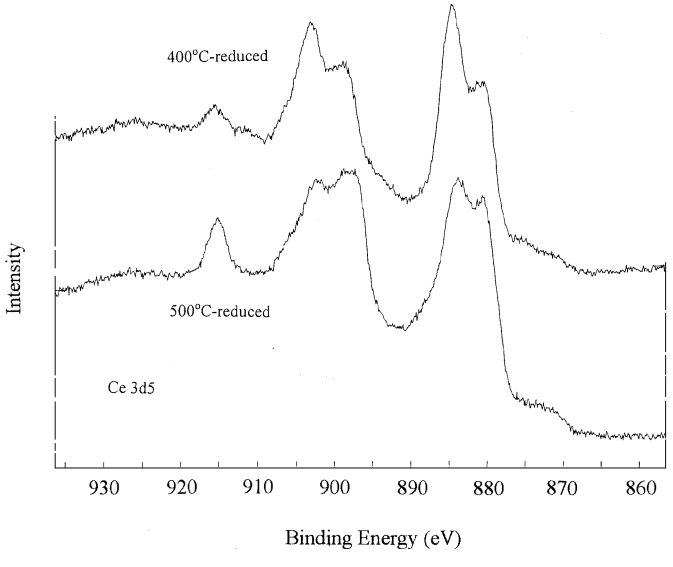

FIG. 1. XPS spectra of cerium in 400°C- and 500°C-reduced Pd/CeO_2 catalysts.

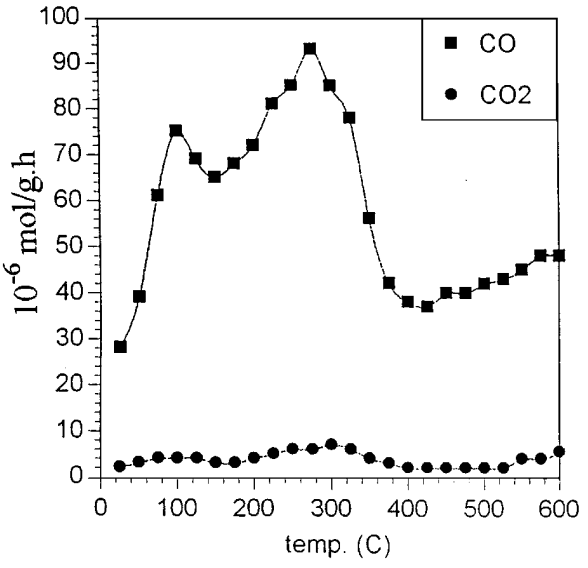

FIG. 2. Temperature programmed desorption profiles of preadsorbed CO_2 on 500°C-reduced Pd/CeO_2 catalysts. Atmosphere, He; rate, 400°C/h.

of Pd and Ce (15). Especially, for CeO_2 support here which has small surface area and low pore volume, this method is believed to be more suitable and accurate. The calculated Pd_{3d}/Ce_{3d} ratio from XPS for 400°C-reduced catalyst was 0.254 while that for 500°C-reduced one was only 0.023, even though the Pd loading is of the same value (Table 1). This result agrees very well with the CO chemisorption result (11), which supports the conclusion that most of the Pd surface is covered by migrated Ce_2O_3 on 500°C-reduced catalyst.

Figure 2 shows the TPD profiles of adsorbed CO_2 in He flow on HTR Pd/CeO_2 catalyst. It is demonstrated that CO_2 could decompose efficiently to form CO at a lower temperature which indicated that Ce_2O_3 was a strong reducing reagent. Trimm *et al.* reported that Ce_2O_3 was so strong a reducing agent that it reduced carbon dioxide to carbon monoxide or even carbon (16, 17). From TPSR profiles of the adsorbed CO_2 in H_2 flow in Fig. 3, CO formed in larger amount than methane, especially at temperatures lower than about 400°C.

Results of CO_2-TPD and CO_2-TPSR experiments showed that CO_2 was adsorbed dissociatively on Ce_2O_3 surface, with the aid from hydrogen spilled over from Pd, to form adsorbed CO and surface oxygen atom. It should be indicated that CO_2 cannot adsorb onto a Pd surface (18). Formed CO shifted to the Pd surface to be hydrogenated there, resulting in methanol formation, while the surface oxygen atom reacted with hydrogen from Pd to form water. Ce_2O_3 formed from reduction of CeO_2 at 500°C had a stronger bonding with adsorbed CO to prevent itself from reoxidation by an adsorbed oxygen atom (19). It is supported by other researchers through IR evidence that adsorbed CO on the Pd surface had a strong CO bond and

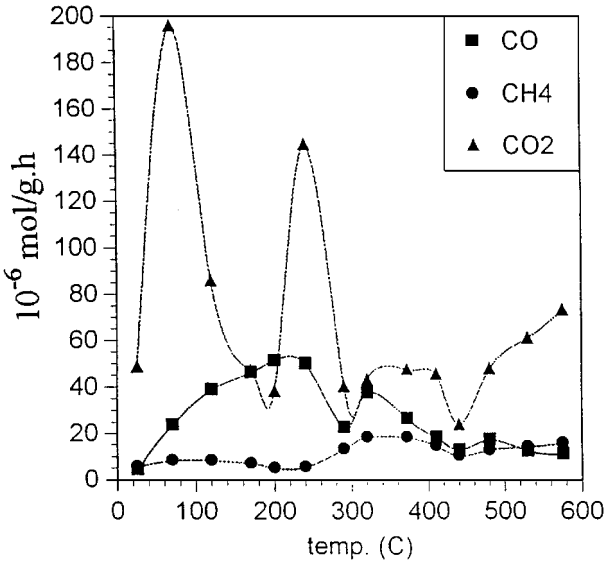

FIG. 3. Temperature programmed surface reaction profiles of preadsorbed CO_2 on 500°C-reduced Pd/CeO_2 catalysts. Atmosphere, H_2; rate, 400°C/h.

a relatively weak Pd–C combination if CO had a large surface coverage ratio on Pd (18, 20). For HTR Pd/CeO_2 here, most of the Pd surface was covered by Ce_2O_3 and Pd was in the form of small domains. Consequently, CO coverage was easily enhanced and the adsorbed CO, with strong CO bond strength, was converted to methanol effectively via a CH_xO intermediate. A stronger CO combination is favorable for the formation of methanol while a weak one prefers methane formation.

CO_2 at 300 Torr was introduced to fresh HTR Pd/CeO_2 catalyst at 230°C for 1 h and the XPS spectra were recorded; and then hydrogen of 300 Torr was successively added to the CO_2-adsorbed catalyst at 230°C for 1 h. Its XPS spectra were recorded by the same way. Figures 4 and 5 compare the spectra. Considering the characteristic peaks of Ce^{3+} (881.6, 898.5 eV) and Ce^{4+} (885.0, 903.8 eV), as demonstrated above in Fig. 1, it is clear that introduction of CO_2 to HTR Pd/CeO_2 resulted in the oxidation of Ce_2O_3. But the cerium oxide formed was not CeO_2 and its valence should be lower than 4 but higher than 3, as exhibited in Fig. 4, where CO_2 adsorption gave an XPS pattern between CeO_2 and Ce_2O_3. In Fig. 4, for high-temperature-reduced Pd/CeO_2, the peak area ratio of A to B (Ce^{4+} to Ce^{3+}) was 6 : 10. When CO_2 was introduced to this catalyst, this ratio changed to 10 : 10, indicating the oxidation of cerium. From Fig. 1, the ratio was 12 : 10 for low-temperature-reduced Pd/CeO_2. Hydrogen introduction made the ratio return to 7 : 10 in Fig. 4.

As CeO_2 is well known as a nonstoichiometric compound and it is considered that exposure of Ce_2O_3 to CO_2 led to the formation of CeO_{2-x} on the surface. Meanwhile, from spectra of C_{1s} as well as O_{1s}, the new peak derived from adsorbed CO appeared in the case of adsorption of CO_2 or $CO_2 + H_2$ onto Ce_2O_3. We conclude that CO_2 decomposed on Ce_2O_3 to form CO and surface oxygen, where the latter combined with Ce_2O_3 to form CeO_{2-x}. It is interesting that hydrogen introduction onto CO_2-adsorbed can remove the oxygen from CeO_{2-x}, resulting in Ce_2O_3 surface oxide, as shown in Fig. 4. The completion of this redox cycle should be critical for the activity and durability of the HTR Pd/CeO_2.

Also from Pd XPS spectra in Fig. 5, it is manifested that CO_2 adsorption on HTR Pd/CeO_2 made the binding energy of Pd shift from 334.8 to 334.2 eV, while $CO_2 + H_2$ adsorption gave 334.4 eV. All of these binding energies are lower than Pd^0 state (335.1–335.5 eV), indicating the electron-rich state of Pd here. As Ce_2O_3 covered a very large part of Pd surface and CO_2 selectively adsorbed onto Ce_2O_3 instead of Pd, electrons should transfer readily from Ce^{3+} to π^* orbital of CO_2 and CO_2 then decomposed to form CO and active surface oxygen (21). At the same time, Ce_2O_3 was oxidized to form CeO_{2-x} here. It is inferred that a part of the electron transfer also occurred between Ce_2O_3 and Pd meanwhile, where electrons shifted from Ce_2O_3 to Pd. Consequently Pd binding energy changed from 334.8 to 334.2 eV. In other

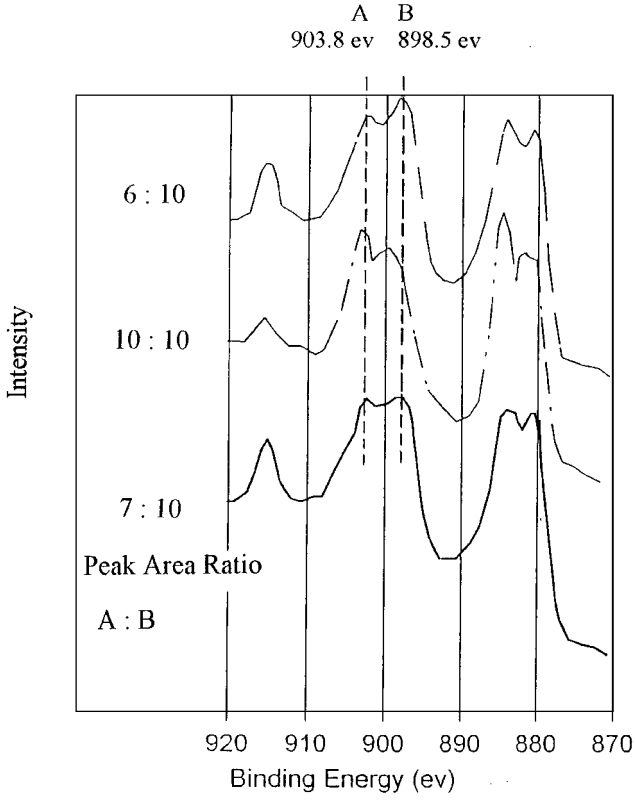

FIG. 4. XPS spectra of cerium in 500°C-reduced Pd/CeO_2 catalysts. Peak area ratios in the figure are relative area ratios for peaks A and B: – –, Pd/CeO_2; – · ·, Pd/CeO_2–CO_2; ———, Pd/CeO_2–CO_2–H_2.

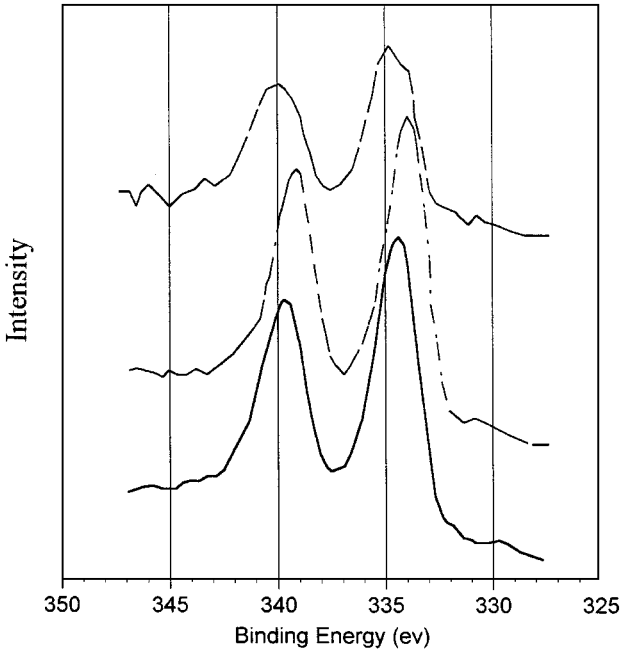

FIG. 5. XPS spectra of palladium in 500°C-reduced Pd/CeO_2 catalysts: – – –, Pd; – · · –, $Pd–CO_2$; ———, $Pd–CO_2–H_2$.

words, CO_2 exposure increased the electron density on Pd through Ce_2O_3. $CO_2 + H_2$ adsorption retarded the electron transfer above. As a result, electron transfer from Ce_2O_3 to Pd became weaker and the Pd binding energy changed moderately from 334.8 eV of HTR Pd/CeO_2 to 334.4 eV. It is considered that under the reaction condition, H_2 can react with surface oxygen species to form water to accomplish a redox cycle of Ce_2O_3 as discussed above, because cerium oxide is known to be effective in water–gas shift reaction through its intrinsic oxygen adjustment ability (22).

We propose the reaction model for CO_2 hydrogenation on the HTR Pd/CeO_2 catalyst, as shown in Fig. 6. Gaseous CO_2 dissociatively adsorbed onto Ce_2O_3 to form CO and oxygen atoms, where Ce_2O_3 covered most of the Pd surface. Oxygen on the Ce_2O_3 surface is very active, due to the activation effect from the coexisting Pd (8, 18). It is also

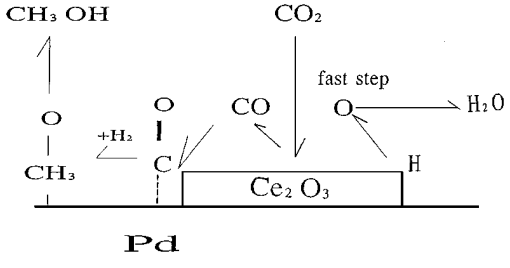

FIG. 6. Reaction model of methanol synthesis from CO_2 and H_2 on 500°C-reduced Pd/CeO_2 catalysts.

possible that the oxygen atom from decomposition of the CO_2 on Ce_2O_3 exchanges with the surface oxygen and bulk oxygen atom of Ce_2O_3 (23). Oxygen atoms reacted with hydrogen spilled over from Pd sites in the vicinity to form water, which kept the Pd and Ce_2O_3 free from oxidation. This decided the long lifetime of this catalyst. CO could shift back to the Pd site, which was at an electron-rich state to adsorb CO strongly, as clarified by XPS.

Other noble metals were used to prepare similar catalysts. The catalyst precursors were $RuCl_3$, $Ni(NO_3)_2$, H_2PtCl_6, respectively. These catalysts were reduced at 500°C in H_2 similarly. Under the same reaction conditions, the Ru catalyst and the Ni catalyst exhibited high methanation activity. On the contrary, the Pt/CeO_x catalyst gave high methanol selectivity, although its level was slightly lower than that of Pd/CeO_x.

Refering to the mechanistic study on Pd/CeO_x, the different reaction results on different metals here provide additional information on the methanol/methane formation site. One can conclude that as the principal intermediate, CO formed on the support and shifted to the metal surface, where methane formation (for Ru or Ni) or methanol formation (for Pd or Pt) occurs, as Ru and Ni are strong to cleave the C–O bond while the Pt and Pd are weak. The spillover behavior of CO here is similar to what was observed on the Pd/La_2O_3 catalyst (24) and alumina-supported noble metal catalysts (25).

Adsorbed CO on Pd surface had a strong CO bond and a relatively weak Pd–C combination if CO had a large CO coverage ratio. As reported by many researchers, one CO molecule combining with two or three Pd surface atoms formed multiple Pd_n–C bond easily in the case of low coverage, giving low IR frequency of adsorbed CO. On the other hand, a mainly linear Pd–CO bond formed in the case of high CO coverage as the Pd surface was covered by a condensed CO layer, exhibiting high IR frequency of adsorbed CO. In other words, the CO bond became strong and the Pd–C combination was weak, while the CO coverage increased (20).

In the HTR Pd/CeO_x catalyst, since most of the Pd surface was covered by Ce_2O_3, the CO coverage was easily enhanced and the adsorbed CO, having a strong CO bond strength, formed methanol effectively via the CH_xO intermediate (21). Since the exposed Pd surface was not so large, being mostly covered by Ce_2O_3, its TOF should be remarkably high.

The reaction on 400°C-reduced Pd/CeO_2 catalyst was conducted where methane was the main product (11). Several previous studies showed that methanation of CO_2 occurred effectively at the interface of the oxide support and noble metal (26). Zhang *et al.* reported that the Rh/TiO_2 catalyst showed high CO selectivity and low CH_4 selectivity if this catalyst was reduced at 500°C and had SMSI effect (26), in good accordance with what was introduced above

on the HTR Pd/CeO_2 catalyst. In our case, CH_3OH was the main product due to the high reaction pressure here. Conversely Zhang *et al.* observed that for low-temperature-reduced Rh/TiO_2 (reduced at 300°C), where SMSI effect was not available, CO selectivity was low and methane selectivity was high. It is further reported by the same group that conversion of CO_2 to CO in the presence of hydrogen is a fast step and happens at the interface of Rh and TiO_2. Similar conclusions were arrived on Ru/TiO_2 catalyst as well, as demonstrated by Prairie *et al.* (27).

CO_2 TPD was conducted on LTR Pd/CeO_2 and it is found that adsorbed CO_2 could not decompose to form CO. TPSR of the adsorbed CO_2 on LTR Pd/CeO_2 was also implemented and it is clear that much methane formed while little CO was detected. On the reaction mechanism, it is considered that CO_2 adsorbed and decomposed to CO and oxygen atom at the interface of Pd and CeO_2 first. This reaction is believed to be available, as proved by published research (26, 27). Formed CO could adsorb onto the Pd surface. Compared to $CO_2 + H_2$ reaction on HTR catalyst, Pd surface was large and in a normal state here. Also the CO formation rate here was lower than that on Ce_2O_3 surface. As a result, CO coverage on Pd surface here was lower than that on HTR catalyst, bringing out the weak CO bond. Large amounts of methane formed while Pd surface was oxidized by the second oxygen atom of CO_2, which was confirmed by XRD for the deactivated catalyst. The deactivation reason for the LTR catalyst on methanol synthesis should be the oxidation of the Pd surface. An alternative route for oxidation of Pd is reverse spillover of the lattice oxygen from ceria to Pd due to the activation effect of Pd on lattice oxygen, as clarified on Rh/Ce_2O_3 (8).

REFERENCES

1. Tauster, S. J., Fung, S. C., and Garten, R. L., *J. Am. Chem. Soc.* **100**, 170 (1978).
2. Tauster, S. J., and Fung, S. C., *J. Catal.* **55**, 29 (1978).
3. Foger, K., *in* "Catalysis, Science and Technology" (J. R. Anderson and M. Boudart, Eds.), Vol. 6, Chap. 4, Springer-Verlag, Berlin, 1984.
4. Haller, G. L., and Resasco, D. E., *Adv. Catal.* **36**, 173 (1989).
5. Hindermann, J. P., Hutchings, G. J., and Kiennemann, A., *Catal. Rev.-Sci. Eng.* **35**, 1 (1993).
6. Datye, A. K., Kalakkad, D. S., Yao, M. H., and Smith, D. J., *J. Catal.* **155**, 148 (1995).
7. de Leitenburg, C., and Trovarelli, A., *J. Catal.* **156**, 171 (1995).
8. Zafiris, G. S., and Gorte, R. J., *J. Catal.* **139**, 561 (1993).
9. Vannice, M. A., *J. Catal.* **40**, 129 (1975).
10. Solymosi, F., Erdohelyi, A., and Kocsis, M., *J. Catal.* **65**, 428 (1980).
11. Fan, L., and Fujimoto, K., *J. Catal.* **150**, 217 (1994).
12. Fleisch, T. H., Hicks, R. F., and Bell, A. T., *J. Catal.* **87**, 398 (1984).
13. Jin, T., and White, J. M., *J. Phys. Chem.* **91**, 5937 (1987).
14. Normand, F. L., *J. Phys. Chem.* **92**, 2561 (1988).
15. Kerkhof, F., and Moulijn, J., *J. Phys. Chem.* **83**, 1612 (1979).
16. Padeste, C., Cant, N., and Trimm, D. L., *Catal. Lett.* **24**, 95 (1994).
17. Padeste, C., Cant, N., and Trimm, D. L., *Catal. Lett.* **18**, 305 (1993).
18. Vannice, M. A., *in* "Catalysis, Science and Technology," Vol. 3, Chap. 3, Springer-Verlag, Berlin, 1982.
19. Arai, T., Maruya, K., Domen, K., and Onishi, T., *J. Catal.* **141**, 533 (1993).
20. Hicks, R. T., and Bell, A. T., *J. Catal.* **90**, 205 (1984).
21. Erdohelyi, A., Cserenyi, J., Papp, E., and Solymosi, F., *Appl. Catal. A* **108**, 205 (1994).
22. Brogan, M. S., Dines, T. J., and Cairns, J. A., *J. Chem. Soc. Faraday Trans.* **90**, 1461 (1994).
23. Che, M., and Tench, A. J., *Adv. Catal.* **32**, 1 (1983).
24. Flesner, R. L., Kester, K. B., Chen, B., and Falconer, J. L., *Stud. Surf. Sci. Catal.* **77**, 277 (1993).
25. Grenoble, D. C., Estadt, M. M., and Ollis, D. F., *J. Catal.* **64**, 90 (1981).
26. Zhang, Z., Kladi, A., and Verykios, X. E., *J. Catal.* **148**, 737 (1994).
27. Prairie, M. R., Renken, A., and Gratzel, M., *J. Catal.* **129**, 130 (1991).